PAPER

CrossMark
click for updates

Donor–acceptor block copolymers carrying pendant PC$_{71}$BM fullerenes with an ordered nanoscale morphology†

Martin Hufnagel,[a] Matthias Fischer,[b] Thomas Thurn-Albrecht[b] and Mukundan Thelakkat*[a]

We present a straightforward method for the preparation of a novel donor–acceptor block copolymer based on an acceptor block with pendant phenyl-C$_{71}$-butyric methyl ester (PC$_{71}$BM) and a regioregular poly(3-hexylthiophene) (P3HT) as a donor. First, a hydroxyl-functionalized polystyrene copolymer with an azide end group was synthesized *via* nitroxide-mediated radical polymerization (NMRP) and was coupled with alkyne-terminated P3HT using copper(I) catalyzed azide–alkyne cycloaddition (CuAAC). The grafting reaction of phenyl-C$_{71}$-butyric acid (PC$_{71}$BA) to the hydroxyl groups of the polystyrene precursor was optimized to yield near-quantitative conversion which is demonstrated for a PC$_{71}$BM-grafted acceptor copolymer in detail using MALDI-TOF mass spectrometry, thermogravimetric analysis (TGA) and ^{1}H-NMR spectroscopy. Owing to the incorporation of C$_{70}$, the donor–acceptor block copolymer exhibits enhanced absorption in the entire visible range of 300 to 600 nm. A detailed structural analysis of the block copolymer based on small-angle X-ray scattering in transmission (SAXS) and in grazing incidence geometry (GISAXS) as well as scanning electron microscopy (SEM) gave clear evidence for the formation of a periodic nanostructure of 37 nm in bulk and in thin films.

Introduction

In the last decade polymeric semiconductors have emerged as a leading class of organic materials with great potential in solution processable, flexible and light-weight organic electronic devices, especially organic photovoltaics (OPV).[1,2] In the case of OPV the physical mixture of a donor and an acceptor material leading to a bulk-heterojunction (BHJ) delivers the highest performance in polymer devices. The short lifetime of excitons in organic semiconductors typically results in a restricted diffusion length of about 10 nm. Moreover the excitons are strongly bound due to Coulomb forces. Therefore, the morphology of the active layer should provide a large donor–acceptor interface with suitable energy levels and small

domain sizes for an efficient charge separation.[3] An interpenetrating network of donor and acceptor materials is additionally essential for charge transport to the electrodes. Thus, controlling the nanostructure in BHJ solar cells is the key to achieve high device performance. The blend morphology of a conjugated polymer and a fullerene derivative was extensively optimized using adequate processing conditions and post-preparation thermal treatments.[4–6] However, such optimized, kinetically frozen mesostructures are in a non-equilibrium state. It is a big challenge to control the size and long-term stability of such mesostructures, which is essential for long-term operational stability.[7,8] These issues become in particular critical for transferring the small area, lab-scale processing of OPV devices to a large scale roll-to-roll fabrication which requires totally different drying or annealing procedures.[9]

An ideal solution to stabilize such a morphology is by the development of nanostructured systems in thermodynamic equilibrium. One of the approaches is by using a single material consisting of both donor and acceptor functions with the capability to self-assemble into the desired nanostructures. Basically, classical coil–coil block copolymers exhibit well-defined equilibrium nanostructures by microphase separation that are tunable in size and shape simply by variation of the degree of polymerization, Flory–Huggins interaction parameter and volume fraction.[10] Theoretical studies on block copolymer

[a]*Applied Functional Polymers, Department of Macromolecular Chemistry I, University of Bayreuth, Universitaetsstr. 30, 95440 Bayreuth, Germany. E-mail: mukundan.thelakkat@uni-bayreuth.de; Fax: +49921-553109; Tel: +49921-553108*

[b]*Experimental Polymer Physics Group, Martin-Luther-Universitaet Halle-Wittenberg, Von-Danckelmann-Platz 3, 06120 Halle, Germany. E-mail: thomas.thurn-albrecht@physik.uni-halle.de; Fax: +49345-5527160; Tel: +49345-5525340*

†Electronic supplementary information (ESI) available: ^{1}H-NMR spectra, UV-Vis spectra, SEC characterization, FTIR spectroscopy data and MALDI-TOF mass spectra. See DOI: 10.1039/c4py01357c

systems comprising donor and acceptor blocks predict an improved device performance for vertically aligned nano-structures.[11] This manuscript deals with the design of fully functionalized donor–acceptor block copolymers with a π-conjugated poly(3-hexylthiophene) (P3HT) and an acceptor block carrying phenyl-C_{71}-butyric methyl ester ($PC_{71}BM$) fullerenes.

Donor–acceptor block copolymers are attractive candidates for single material solar cells.[12,13] Typically, P3HT is employed as the donor block and perylene bisimides (PBI) or fullerenes as acceptor units. We have recently reported well-defined microphase separation in P3HT-*b*-poly(PBI) active donor–acceptor block copolymers with a lamellar or cylindrical morphology in the range of tens of nanometers.[14] Since fullerenes are known to be so far the most efficient acceptor material in OPV, it seems reasonable to integrate fullerenes into donor–acceptor block copolymers, which has been realized by grafting C_{60} and its derivatives using different synthetic approaches. The very first study on block copolymers carrying a conjugated block and a fullerene pendant block was reported by Hadziioannou *et al.*[15]

Perrin *et al.* showed that the unique electron-acceptor/transporting capability of fullerenes is maintained in C_{60}-grafted polymers.[16] Just recently, we could demonstrate a well-defined synthesis method for fullerene-grafted copolymers carrying phenyl-C_{61}-butyric methyl ester ($PC_{61}BM$) which shows high electron mobilities up to 1×10^{-4} cm V^{-1} s^{-1} without the formation of nanocrystals.[17]

Many of the synthetic strategies which aim at a covalent attachment of fullerenes to the block copolymer rely on reactions with unmodified C_{60} fullerenes. For example, atom transfer radical addition (ATRA),[18] [3 + 2]-cycloaddition with azides[19,20] or routes using tosylhydrazone addition[21] to C_{60} have been reported. Since buckminsterfullerene C_{60} can act as a multifunctional reactant these methods often lead to polymer crosslinking by multiple additions and result in diminished solubility of the products. More complex mono-functional fullerenes have been attached to block copolymers in an azide–alkyne Huisgen cycloaddition[22,23] or Williamson ether synthesis.[24] Lee *et al.* have reported a Steglich esterification procedure using phenyl-C_{61}-butyric acid ($PC_{61}BA$)[25] which is easily accessible from commercially available $PC_{61}BM$ in a straightforward acidic hydrolysis.[26] Another concept toward donor–acceptor copolymers with graft-type architecture has been reported by Sivula *et al.* based on ring opening meta-thesis polymerization of C_{60}- and P3HT-bearing norbornene monomers.[27] Even though different synthetic approaches to realize fullerene containing block copolymers as discussed above have been reported, no long range microphase separation has been observed for C_{60}-grafted donor–acceptor block copolymers so far.[28] An additional issue of C_{60} fullerenes is their low optical density and thus C_{60} does not contribute substantially to light harvesting. But C_{70} and its derivatives absorb much more efficiently in the visible range, which considerably improves the photocurrent in solar cells.[29] Therefore, $PC_{71}BM$ is the state-of-the-art acceptor material in OPV exhibiting record efficiencies[30] and it is desirable to incorporate C_{70}

fullerenes also into donor–acceptor block copolymers. To the best of our knowledge there are no reports regarding the grafting of C_{70} into fully functionalized donor–acceptor block copolymers.

Taking into account the above facts we address the following questions in the design and structure elucidation of $PC_{71}BM$-grafted donor–acceptor block copolymers: 1. What are the optimum reactions conditions for an efficient grafting of $PC_{71}BM$ into a polystyrene backbone? 2. Is it feasible to incorporate $PC_{71}BM$ into a donor–acceptor block copolymer maintaining the high solubility and high yield of grafting? 3. Does such a block copolymer self-assemble into a periodic donor–acceptor nanostructure?

In this work we present the high yield grafting of $PC_{71}BM$ to obtain $PC_{71}BM$-grafted copolymers ($PPC_{71}BM$) and the controlled synthesis of a P3HT-*b*-$PPC_{71}BM$ donor–acceptor block copolymer. Furthermore, we study the structure formation of this block copolymer using X-ray scattering methods and scanning electron microscopy.

Results and discussion

Our synthetic strategy for P3HT-*b*-$PPC_{71}BM$ is based on copper(I) catalyzed azide–alkyne cycloaddition (CuAAC) of two individually designed polymer blocks: a hydroxyl functionalized polystyrene copolymer with an azide end group and a P3HT-alkyne. This was followed by a Steglich esterification procedure using phenyl-C_{71}-butyric acid ($PC_{71}BA$) to obtain the target donor–acceptor block copolymers (Fig. 1). A major challenge in block copolymer synthesis *via* CuAAC is the control over the end group functionalization of both polymer blocks. In the case of P3HT-alkyne, high end group fidelity was achieved by termination of the Kumada transfer catalyst polymerization with ethynylmagnesium chloride.[31] For the synthesis of the azide-terminated polystyrene precursor a statistical copolymer, poly(4-methoxystyrene-*stat*-4-*tert*-butoxystyrene), was used. This was achieved by nitroxide-mediated radical polymerization (NMRP) and a subsequent polymer-analogous introduction of
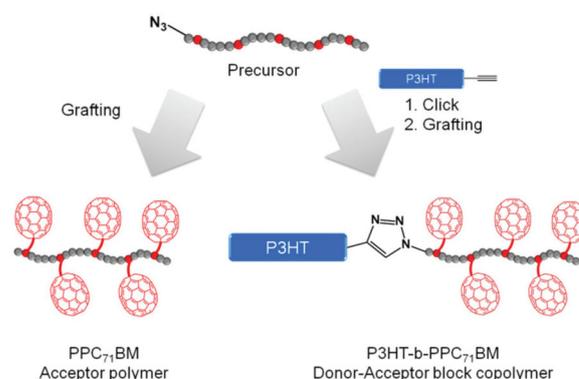
Fig. 1 Schematic representation of the synthetic strategies toward $PC_{71}BM$-grafted acceptor polymers and donor–acceptor block copolymers.
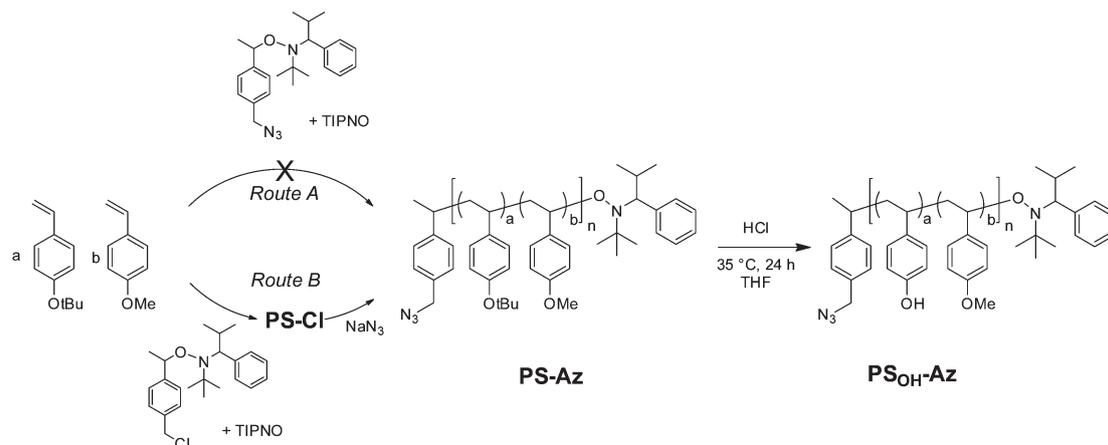
Scheme 1 Synthesis strategy toward the azide-terminated precursor copolymer poly(4-methoxystyrene-*stat*-4-hydroxystyrene). Introduction of the azide end group is attempted by two different methods depicted as routes A and B. The hydroxyl functionality is achieved by hydrolysis of the *tert*-butyl ether groups in PS-Az maintaining the azide end group to obtain PS$_{OH}$-Az.

an azide end group. The NMRP copolymers proved to be highly tolerant toward polymer-analogous reactions.

Hydroxyl-functionalized polystyrene copolymers with azide end groups

We examined two synthetic strategies toward azide terminated copolymers using NMRP (Scheme 1): route A is intended to introduce the azide group to the copolymer directly through an azide derivatized alkoxyamine initiator. Route B is based on two steps involving copolymerization with a chloride derivatized initiator and a subsequent polymer-analogous substitution with sodium azide (route B).

For both routes the feed ratio of 4-*tert*-butoxystyrene (BS) and 4-methoxystyrene (MS) BS : MS was $a : b = 0.08 : 0.92$ and gave the copolymer poly(4-methoxystyrene-*stat*-4-*tert*-butoxy-styrene) (PS) with a built-in ratio of $a : b = 0.10 : 0.90$, which can be extracted from ^{1}H-NMR analysis (Fig. S1†). The particular ratio was selected to realize a ratio of 1 : 1 w/w of P3HT and PC$_{71}$BM in the final block copolymer which is reported to be optimum for charge separation and transport.[32]

In route A, the styrene monomers were copolymerized using the azide-functionalized alkoxyamine initiator 2,2,5-trimethyl-3-(1′-*p*-azidemethylphenylethoxy)-4-phenyl-3-azahexane (Ini-Az) and 2,2,5-trimethyl-4-phenyl-3-azahexane-3-nitroxide (TIPNO) as persistent radical (Scheme 1). The copolymerization was carried out at 125 °C in *o*-dichlorobenzene (DCB) solution. The copolymerization follows a statistical incorporation of the monomers according to the evaluation of samples which were periodically taken during the copolymerization.

Here, the consumption of both monomer species BS and MS proved to be equally fast. This can be deduced from the ^{1}H-NMR spectra at different polymerization times (*i.e.* conversions), where the ratio of residual monomers in the reaction mixture remains constant (Fig. S2†). The size-exclusion chromatography (SEC) trace of PS shows a number-averaged molecular weight (M_n) of 19.6 kg mol^{-1} with a polydispersity (PDI) of 1.19 (Fig. 2a). The slightly broad molecular weight
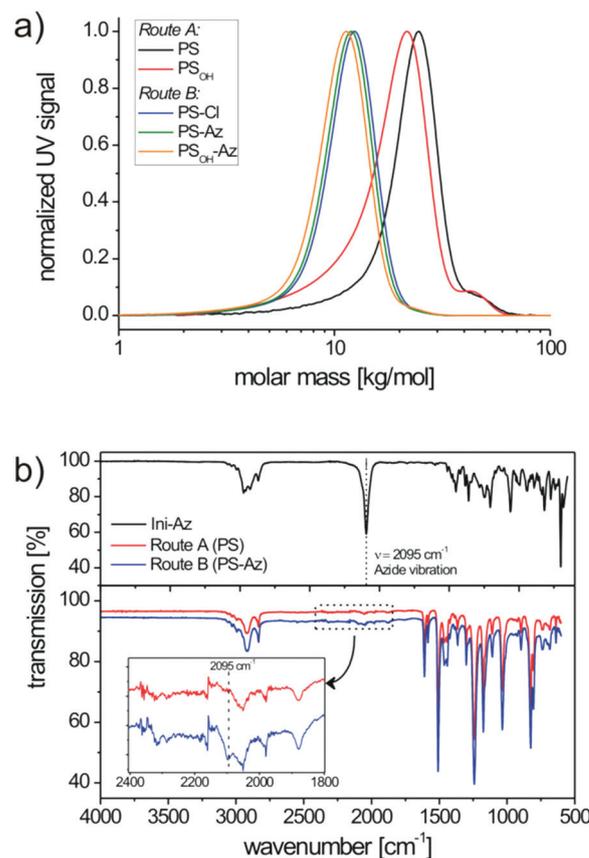
Fig. 2 SEC traces (a) of the copolymers from route A (PS and PS$_{OH}$) and route B (PS-Cl, PS-Az and PS$_{OH}$-Az) obtained by NMRP. Corresponding FTIR spectra (b) of the copolymers demonstrate the degree of azide end group functionalization.

distribution results from a shoulder at roughly double molecular weight and can be assigned to a small amount of radical recombination of polymer chains. To verify the azide end group fidelity, Fourier-transform infrared (FTIR) spectroscopy

was performed. This analytical method is highly sensitive for the detection of organic azides since the asymmetric vibration of azides is very strong.[33] Unlike the azide initiator Ini-Az, the copolymer from route A does not show a distinct azide vibration at 2095 cm^{-1} (Fig. 2b). In the literature it has been proposed that the azide end group of the alkoxyamine initiator can react in an azide–alkene cycloaddition during polymerization with the styrene monomers at 125 °C.[34] This explains the lack of FTIR azide vibrations in the copolymer from route A. Additionally, this is supported by our observation that the polystyrene copolymers from route A did not form any block copolymer using click chemistry.

In route B, the copolymerization was performed in bulk in the presence of the chlorine-functionalized alkoxyamine initiator 2,2,5-trimethyl-3-(1′-p-chloromethylphenyl-ethoxy)-4-phenyl-3-aza-hexane (Ini-Cl) and TIPNO (Scheme 1). Here also the feed ratio of BS : MS was 0.08 : 0.92 and copolymerization until 40% conversion gave a chlorine-terminated polystyrene copolymer (PS-Cl) with a built-in ratio of BS : MS = 0.10 : 0.90 (Fig. S3†). Bulk polymerization improved the copolymerization and no high molecular weight shoulder could be observed in SEC analysis (Fig. 2a). This polymerization procedure enables a perfect control of the statistical copolymerization with mono-modal molecular weight distribution and a very low poly-dispersity of 1.10. PS-Cl has a molecular weight of M_n = 9.8 kg mol^{-1} (Fig. 2a). In a subsequent step, the chloride end group of PS-Cl was replaced in a nucleophilic substitution reaction using an excess of sodium azide. The resulting azide-monoterminated copolymer PS-Az has a molecular weight of M_n = 10.4 kg mol^{-1} and a narrow polydispersity of 1.10 (Fig. 2a). In contrast to route A, the copolymer PS-Az from route B shows an azide vibration at 2095 cm^{-1}. As expected, the observed signal is weak due to the high dilution of the end group. This indicates a successful end group functionalization with azide via the polymer-analogous substitution in route B. Additionally, the FTIR spectra of PS-Cl and PS-Az are compared in Fig. S4† which also confirm the successful conversion of the halide to azide.

The next step toward the hydroxyl-functionalized poly-(4-methoxystyrene-stat-4-hydroxystyrene) precursor copolymer (PS$_{OH}$-Az) is the deprotection of the tert-butoxystyrene repeating units. Under acidic conditions with hydrochloric acid at a mild temperature of 35 °C, the cleavage of the tert-butylether groups is usually quantitative.[17] This was evidenced by ^{1}H-NMR, where the hydroxyl signal at δ = 9.24–8.84 ppm indicates the successful hydrolysis of the tert-butoxystyrene units (Fig. S5†). The obtained copolymer PS$_{OH}$-Az exhibits a molecular weight of M_n = 9.8 kg mol^{-1} and a narrow monomodal distribution with a PDI of 1.11 (Fig. 2a). The precursor copolymer carries 10 mol% of 4-hydroxystyrene units which can be used for the esterification with PC$_{71}$BA.

Optimized fullerene grafting with PC$_{71}$BA

To find the optimum conditions for the covalent PC$_{71}$BM fullerene attachment via Steglich esterification, we tested the grafting reaction using a hydroxyl-functionalized polystyrene
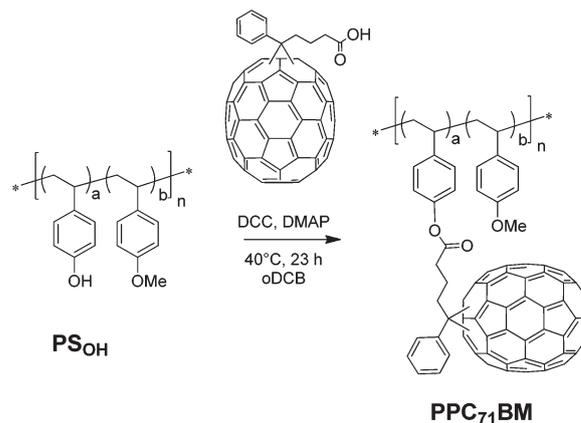
Scheme 2 Monofunctional grafting of the precursor copolymer PS$_{OH}$ via Steglich esterification with PC$_{71}$BA.

copolymer PS$_{OH}$ obtained via NMRP having a molecular weight of M_n = 16.7 kg mol^{-1}, PDI = 1.19 and containing 10 mol% hydroxystyrene. As a fullerene derivative we synthesized the monofunctional reactant phenyl-C$_{71}$-butyric acid (PC$_{71}$BA) by hydrolysis of the commercially available phenyl-C$_{71}$-butyric acid methyl ester (PC$_{71}$BM) in analogy to a protocol from Hummelen et al.[26] Generally, toxic solvents such as carbon disulfide (CS$_2$) are used for reactions involving PC$_{61}$BA. Owing to the increased solubility of PC$_{71}$BA (1.48 mg mL^{-1}) compared to PC$_{61}$BA (0.38 mg mL^{-1}) in DCB, we were able to avoid CS$_2$. Even then the grafting yield was very high (Scheme 2).

The esterification of PS$_{OH}$ was carried out in DCB at 40 °C for 23 h in the presence of an excess of PC$_{71}$BA (2 equivalents with respect to the hydroxyl groups) and N,N′-dicyclohexyl carbodiimide (DCC) and 4-dimethylaminopyridine (DMAP). The crude product was purified by an extensive procedure to guarantee that only covalently bound fullerenes remain in the product (see the Experimental part). The low molecular weight fullerene side products (e.g. N-acyl urea derivatives) were removed by several precipitation cycles into mixtures of methanol : toluene (1 : 2, v : v). The purity of the PC$_{71}$BM-grafted copolymer PPC$_{71}$BM was monitored by thin layer chromatography (TLC), where the small molecule impurities appear as distinct spots. Further, the ^{1}H-NMR spectrum (Fig. S6†) verifies the purity of PPC$_{71}$BM, since any low-molecular weight fullerene impurity would appear as sharp multiplets in the spectrum. The obtained polymer PPC$_{71}$BM is highly soluble in chlorinated solvents such as chloroform, chlorobenzene and DCB. The grafted product was further analyzed using ^{1}H-NMR to verify the grafting reaction.

The ^{1}H-NMR spectrum of PPC$_{71}$BM clearly supports a successful grafting reaction since all relevant resonances belonging to the polymer and the pendant fullerenes are present in the product (Fig. S6†). The multiplets of methylene protons of the pendant PC$_{71}$BM appear as strongly broadened signals indicating a successful covalent linkage to the polymer backbone. SEC analysis in chloroform as an eluent shows a molecular weight of M_n = 20.8 kg mol^{-1} and a relatively narrow

distribution with PDI = 1.27 (Fig. S7†). Note that there is no polymer crosslinking observed in the SEC trace; there is only the shoulder at higher molecular weight which was already present in the precursor PS_{OH}. The peak maximum in SEC increased from 21.7 kg mol^{-1} for PS_{OH} to 26.3 kg mol^{-1} for $PPC_{71}BM$. It is typical of fullerene polymers that the effective molecular weight is underestimated in SEC, most probably due to strong intrachain interactions between the pendant fullerene moieties.[15]

To quantify the extent of fullerene grafting, we favor matrix assisted laser desorption ionization mass spectrometry with time of flight detection (MALDI-TOF MS) as a very reliable method.[17] The mass spectra of the precursor copolymer PS_{OH} and the grafted copolymer $PPC_{71}BM$ are depicted in Fig. 3a. Here, the esterification leads to a significant mass increase of the copolymer due to the pendant fullerenes from $M_p =$ 24.4 kg mol^{-1} for PS_{OH} to $M_p = 42.4$ kg mol^{-1} for $PPC_{71}BM$. M_p denotes the peak maximum of the molar mass distribution curve. The resulting mass increase, ΔM, is 18.0 kg mol^{-1} and this corresponds to the amount of attached $PC_{71}BA$ per polymer chain. From M_p of PS_{OH} we can further estimate the average degree of polymerization, which is 181 repeating units per chain. Since the copolymer PS_{OH} contains 10 mol% hydroxystyrene, the number of hydroxyl groups is 18 units on an average. Therefore, a maximum of 18 $PC_{71}BA$ moieties ($M =$ 1016.99 g mol^{-1}) can be grafted per chain which corresponds to a theoretical mass increase of 18.3 kg mol^{-1}. From this, we deduce that the efficiency of grafting is almost quantitative (98%) and yields a copolymer with 42 wt% of pendant $PC_{71}BM$. Thermogravimetric analysis (TGA) of the polymers PS_{OH} and $PPC_{71}BM$ fully supports these findings (Fig. 3b). Whereas the precursor copolymer PS_{OH} is decomposed almost completely in nitrogen, the fullerene-grafted $PPC_{71}BM$ shows a significant amount of residual char. This residue corresponds to the C_{70} fullerene core which is thermally very stable and does not decompose until 800 °C. Thus, we can roughly estimate the fullerene weight content of $PPC_{71}BM$ as 49 wt%. This is in very good agreement with the MALDI-TOF MS result since the content of PCBM in TGA is usually overestimated, likely due to incomplete decomposition.[17]

The optical absorption of $PPC_{71}BM$ ranges from the UV region to 650 nm and, hence, has an improved light harvesting capability with respect to optical density and wavelength range compared to the known C_{60} fullerene polymers. This was confirmed by UV-vis spectroscopy in solution (Fig. S8†).

Since $PC_{71}BM$ is a crystalline material, we were also interested in knowing whether the covalent attachment of these fullerene moieties to the copolymer backbone influences the crystallization or not. X-ray diffraction of a powder sample prepared by slow evaporation of a solution of $PPC_{71}BM$ in DCB confirmed the absence of any fullerene crystallites showing only an amorphous scattering signal (Fig. S9†). This is very similar to the observation of amorphous states in $PPC_{61}BM$ polymers.[17] This is also an important aspect regarding structure formation in block copolymers comprising a $PPC_{71}BM$ block, because a too strong fullerene interaction may disturb the self-assembly of the block copolymer, which is not the case here.

Synthesis and characterization of the donor–acceptor block copolymer with pendant $PC_{71}BM$

The target block copolymer was obtained by a polymer–polymer click reaction followed by the grafting of $PC_{71}BM$ onto the PS backbone (Scheme 3). For the click reaction, ethynyl end-capped P3HT having an average molecular weight of $M_n =$ 19.2 kg mol^{-1} (SEC) and a narrow polydispersity of 1.11 (Fig. 4a) and the PS_{OH}-Az with 9.8 kg mol^{-1} and polydispersity of 1.11 were used. P3HT with a molecular weight M_n around 20 kg mol^{-1} (SEC) exhibits optimum charge transport[35] and can promote phase separation in block copolymers due to its high degree of polymerization.[14] The copolymer PS_{OH}-Az contains 10 repeating units of 4-hydroxystyrene and therefore can be grafted with up to 10 kg mol^{-1} $PC_{71}BM$. This yields roughly equal amounts of donor and acceptor compounds in the final block copolymer, which is in analogy to the ratio typically used in blend solar cell devices.[32]

The CuAAC reaction was carried out with ethynyl-end-capped P3HT and three equivalents of azide-terminated PS_{OH}-Az in the presence of copper(ı) iodide/N,N,N',N',N''-penta-methyl-diethylenetriamine (PMDETA) as a catalyst (Scheme 3).
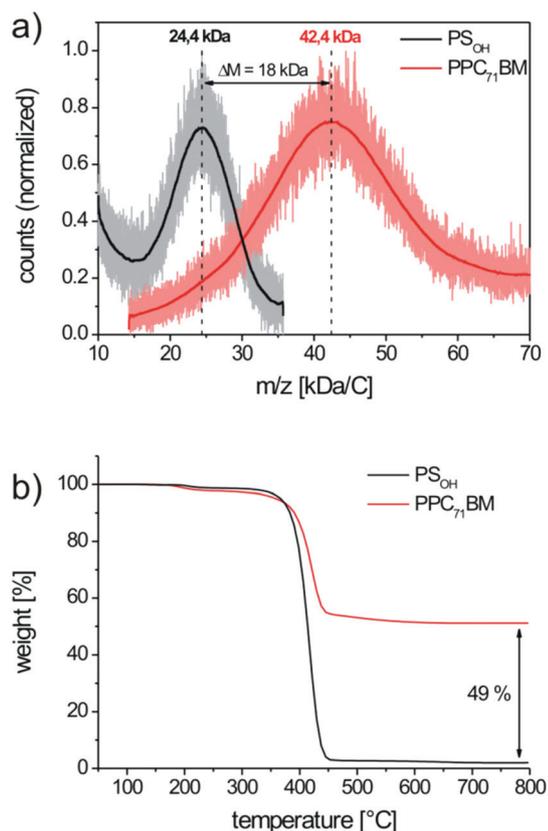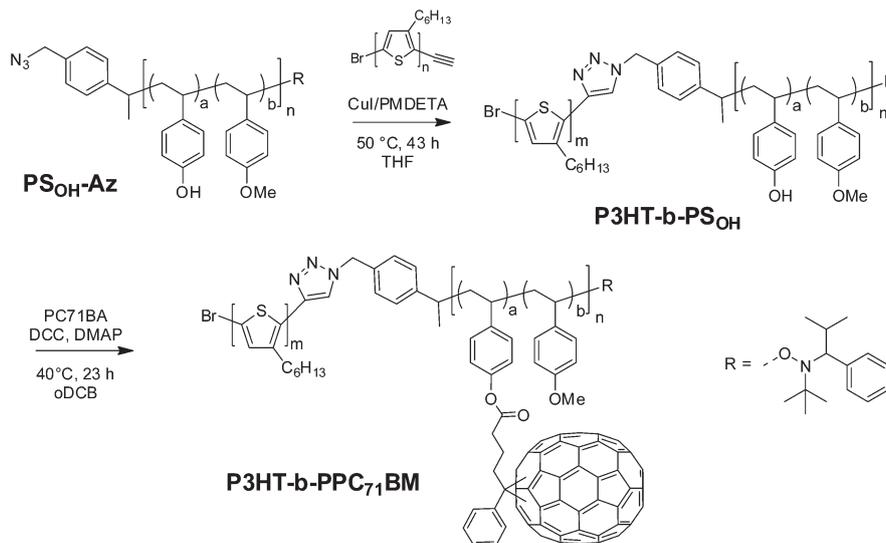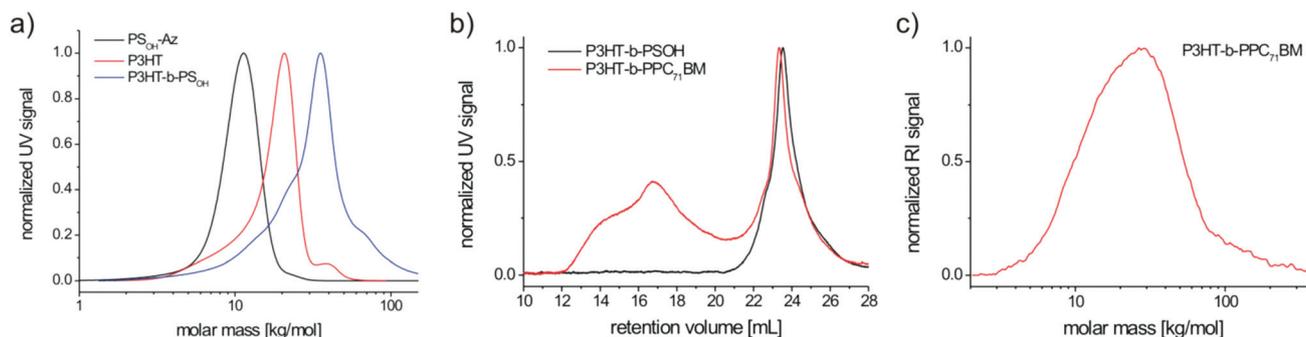

Fig. 3 Determination of the $PC_{71}BM$ content in $PPC_{71}BM$ by (a) MALDI-TOF mass spectrometry and (b) by thermogravimetric analysis in nitrogen atmosphere.

Scheme 3 Synthesis route of the donor–acceptor block copolymer P3HT-*b*-PPC$_{71}$BM *via* polymer–polymer click chemistry and Steglich esterification with PC$_{71}$BA.

Fig. 4 SEC traces of (a) the polymer–polymer coupling by click chemistry (THF, UV detector). Analysis of the block copolymer P3HT-*b*-PS$_{OH}$ and P3HT-*b*-PPC$_{71}$BM *via* SEC in chloroform (b) and SEC in 1,2,4-trichlorobenzene at 150 °C for P3HT-*b*-PPC$_{71}$BM (c).

The precursor PS$_{OH}$-Az was used in excess, since it can be separated easily from the block copolymer afterwards by precipitation in a mixture of methanol : acetone (2 : 1/v : v). We monitored the progress of block copolymer formation by SEC and stopped the reaction after 43 hours, when no further consumption of P3HT could be observed.

From the SEC traces shown in Fig. 4 it is obvious that the polymer–polymer click reaction was successful resulting in the diblock copolymer P3HT-*b*-PS$_{OH}$ with an average molecular weight M_n of 26.3 kg mol^{-1} and a polydispersity of 1.35. The broad polydispersity can be accounted for by taking into consideration the residual P3HT homopolymer observed as a shoulder in the SEC trace (Fig. 4a). This can be attributed to either an incomplete click reaction and/or an insufficient ethynyl functionalization of P3HT. The small shoulder at higher molecular weight of the block copolymer SEC trace might be due to aggregation effects in SEC.

The composition of the block copolymer P3HT-*b*-PS$_{OH}$ can be deduced from the individual blocks that were analyzed by MALDI-TOF MS (Fig. S10†). Here, the mass spectrum of P3HT

shows a major peak series corresponding to the ethynyl-P3HT (Fig. S10a†) with an M_p of 12.4 kg mol^{-1} which is equal to 74 hexylthiophene repeating units (RU). The mass spectrum of PS$_{OH}$-Az (Fig. S10b†) shows an M_p of 13.4 kg mol^{-1} which corresponds to 98 repeating units in the copolymer. Thus, for P3HT-*b*-PS$_{OH}$ we can expect a peak molecular weight of 25.8 kg mol^{-1}. Exactly the same molecular weight is found for the P3HT-*b*-PS$_{OH}$ block copolymer (25.9 kg mol^{-1}). Therefore, the MALDI-TOF mass spectrum analysis unambiguously proves the success of the polymer–polymer click reaction (Fig. S10c†). To summarize, P3HT-*b*-PS$_{OH}$ on average contains 74 RU of hexylthiophene and 98 RU of styrene moieties (Table 1). Taking into consideration the composition of the PS$_{OH}$ block ($a : b = 0.10 : 0.90$), a total number of ten 4-hydroxystyrene (HS) units per block copolymer chain is present. The composition of the block copolymer P3HT-*b*-PS$_{OH}$ was also verified using ^{1}H-NMR analysis. We can find all relevant proton resonances in the ^{1}H-NMR spectrum of P3HT-*b*-PS$_{OH}$ (Fig. S11†). From the integral ratio of the thiophene proton singlet at $\delta = 7.37$ ppm and the broad phenyl proton multiplet

Table 1 Experimentally determined molecular weight data of the block copolymers and its contributing polymer blocks

| Polymer | SEC | | MALDI[c] | DP | |
	M_n [kg mol^{-1}]	PDI	M_p[d] [kg mol^{-1}]	m	n
PS$_{OH}$-Az[a]	9.8	1.11	13.4	—	98[f]
P3HT-alkyne[a]	19.2	1.11	12.4	74[g]	—
P3HT-b-PS$_{OH}$[a]	26.3	1.35	25.9	74[h]	103[h]
P3HT-b-PPC$_{71}$BM[b]	27.5	1.31	31.5[e]	74[h]	102[h]

[a] SEC in tetrahydrofuran as an eluent, a UV (254 nm) detector, polystyrene calibration. [b] SEC in chloroform as an eluent, a UV (254 nm) detector, polystyrene calibration excluding the aggregation region. [c] Matrix-assisted laser desorption/ionization mass spectrometry with time of flight detection. [d] M_p is the peak maximum of the molecular weight distribution curve. [e] M_p determined from the very broad mass distribution. [f] Degree of polymerization (DP) determined from M_p of the MALDI-TOF mass spectrum. [g] DP determined from M_n = 12.3 kg mol^{-1} of MALDI-TOF MS. [h] DP determined from the ^{1}H-NMR spectrum.

at δ = 7.11–6.52 ppm we calculated the composition of P3HT-b-PS$_{OH}$ of m : n = 74 : 103 repeating units. Thus, the composition of the block copolymers deduced from NMR is in very good agreement with the MALDI-TOF MS data for the individual polymer blocks.

In the final step of polymer-analogous grafting we attached PC$_{71}$BA to P3HT-b-PS$_{OH}$ by Steglich esterification. Similar reaction conditions using DCC and DMAP in dichlorobenzene as those for PPC$_{71}$BM were used here. The applied amount of PC$_{71}$BA with respect to hydroxyl groups in P3HT-b-PS$_{OH}$ was adjusted to approximately 2.5 equivalents to obtain a high degree of grafting. The product was extensively purified by several precipitations into methanol : toluene (1 : 1, v : v) and pure methanol. The removal of small molecule fullerene side products was thoroughly monitored via TLC. Furthermore, the absence of multiplet resonances for fullerene side products is supported by ^{1}H-NMR in deuterated DCB (Fig. S12†). This NMR solvent turned out to give the most reasonable spectra because aggregation of the P3HT-b-PPC$_{71}$BM in chloroform is also a challenging problem for NMR analysis. The spectrum exhibits all the expected signals corresponding to both P3HT and PPC$_{71}$BM blocks. Comparing the ratio of the thiophene protons at δ = 7.36 ppm (1H) with the phenyl protons of the polystyrene block at δ = 7.09–6.51 ppm (4H) we obtain a ratio of repeating units of P3HT and polystyrene of m : n = 74 : 102, which is very close to the expected ratio of 74 : 98 from MALDI-TOF MS analysis. The pendant fullerene proton resonances are rather weak in the aromatic region at δ = 7.94–7.86 ppm and δ = 7.70–7.46 ppm and, additionally, strongly overlap in the case of the methylene resonances.

A significant tendency of P3HT-b-PPC$_{71}$BM toward aggregation in chloroform is observed in the SEC eluogram of Fig. 4b. While P3HT-b-PS$_{OH}$ exhibits a rather narrow and monomodal eluogram, P3HT-b-PPC$_{71}$BM is characterized by a sharp peak at 23.34 mL corresponding to the fully dissolved block copolymer and a huge amount of aggregates at very low retention volumes. The aggregation can be suppressed at elevated temp-

erature and by changing the eluent, which is demonstrated by high-temperature SEC in 1,2,4-trichlorobenzene at 150 °C (Fig. 4c). Here, the SEC trace shows a monomodal mass distribution in the expected mass range. Using a polystyrene calibration, the molecular weights of P3HT-b-PS$_{OH}$ and P3HT-b-PPC$_{71}$BM correspond to M_n = 26.3 kg mol^{-1} (M_p = 34.3 kg mol^{-1}) and M_n = 27.5 kg mol^{-1} (M_p = 36.6 kg mol^{-1}) respectively (Table 1). This expected marginal molecular weight shift in SEC is in full agreement with the contractile effects of fullerene polymers (see also PPC$_{71}$BM).

To quantify the exact composition of the donor–acceptor block copolymer P3HT-b-PPC$_{71}$BM we applied UV-vis spectroscopy in solution and MALDI-TOF MS. The mass spectrum of P3HT-b-PPC$_{71}$BM in Fig. S10c,† however, is not suited to derive a clear composition of donor and acceptor blocks. Here, not only a shift toward higher molecular weight indicating a covalent grafting with PC$_{71}$BA, but also a broadening of the mass distribution is observed.

A very useful method for the estimation of the PC$_{71}$BM content is UV-vis spectroscopy. It is possible to calculate the content of a chromophore in polymers by comparing the extinction coefficients of polymers and the pure chromophore as a reference in dilute solutions.[17,36]

To determine the PC$_{71}$BM content, we used the extinction coefficients of PC$_{71}$BM and P3HT-b-PPC$_{71}$BM at 274 nm (Fig. 5a), at which PC$_{71}$BM shows a shoulder with high optical density. For the calculation, the residual absorption of polystyrene and P3HT at this wavelength was subtracted. Details of the exact calculation of the PC$_{71}$BM content in the block copolymer are given in the ESI.† According to our calculations, the block copolymer P3HT-b-PPC$_{71}$BM contains 24 wt% of PC$_{71}$BM. Taking into consideration the MALDI TOF MS value of P3HT, the composition of P3HT to PC$_{71}$BM was obtained as 1 : 0.86. The maximum possible theoretical content of PC$_{71}$BM can be estimated based on the MALDI molecular weights of the individual polymer blocks (12.4 kg mol^{-1} for P3HT, 13.4 kg mol^{-1} for PS$_{OH}$) and the maximum possible grafting which is supposed to be ten PC$_{71}$BM units per polymer chain with a total weight of 10.17 kg mol^{-1}. This results in a theoretical PC$_{71}$BM content of 28 wt%. Comparing the theoretical PC$_{71}$BM content of 28 wt% in P3HT-b-PPC$_{71}$BM with the experimental value of 24 wt% from UV-vis, we can conclude a very high grafting efficiency of 86%.

UV-Vis absorption studies of thin films allow for a qualitative estimation of the crystallization of P3HT (Fig. 5b). The neat P3HT shows distinct absorption bands at about 520, 560 and 605 nm which are ascribed to the formation of weak H-aggregates in crystals,[37] whereas the amorphous P3HT phase exhibits a non-structured absorption band with a peak maximum at 450 nm. Both the block copolymers P3HT-b-PS$_{OH}$ and P3HT-b-PPC$_{71}$BM exhibit the typical absorption bands relevant for aggregates or crystallites, but the relative intensities of the aggregate bands are lower compared to that of neat P3HT. On annealing P3HT-b-PPC$_{71}$BM at 160 °C for 2 hours the aggregate bands appear more pronounced. On the other hand, heating the sample just above the melting point of
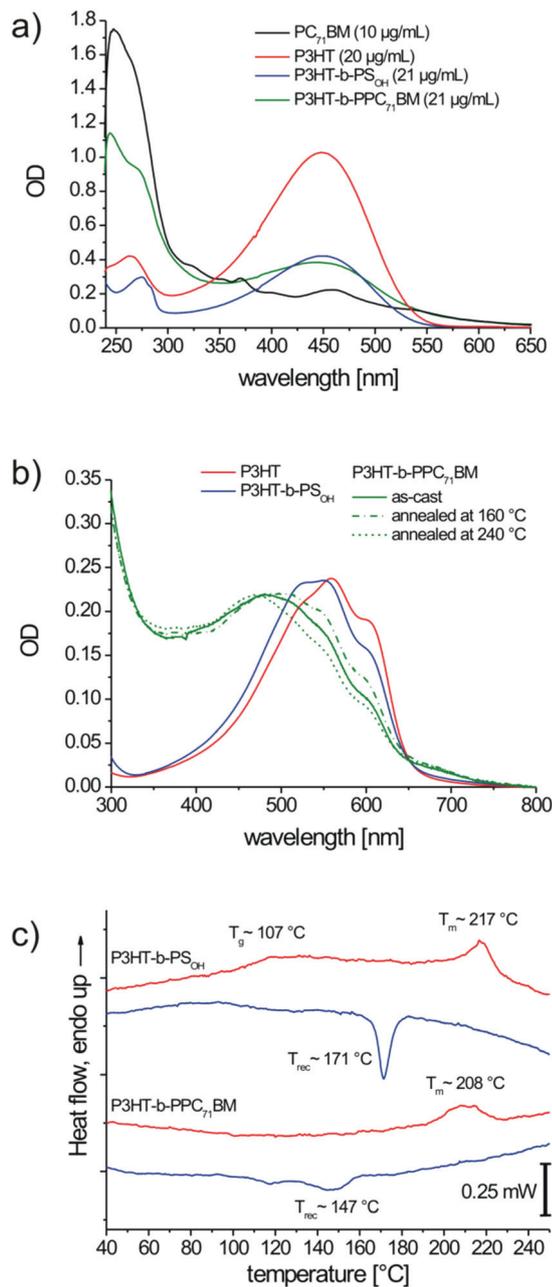
Fig. 5 UV-vis absorption spectra (a) taken from solutions in chloroform. The spectra of $PC_{71}BM$ and P3HT are given as references and for the determination of the mass fractions of P3HT and $PC_{71}BM$ incorporated into the block copolymers. UV-vis spectra of thin films (b) after spin-coating (solid lines) and for P3HT-b-$PPC_{71}BM$ additionally after thermal annealing for 2 hours at 160 °C (dash-dot) and after annealing at 240 °C with a subsequent cooling rate of approximately 10 K min^{-1} (short dash). Differential scanning calorimetry traces (c) of the block copolymers P3HT-b-PS_{OH} and P3HT-b-$PPC_{71}BM$. The DSC traces for the heating cycles are red and blue for the cooling cycles.

P3HT (240 °C) and cooling at 10 K min^{-1} (similar to DSC cooling scan) there is a reduction of intensity of the aggregate bands. This clearly indicates that appropriate annealing procedures need to be developed for the crystallization of P3HT in the block copolymers.

Differential scanning calorimetry (DSC) confirms that P3HT-b-PS_{OH} contains a crystalline P3HT block with a peak melting temperature of 217 °C and a melting enthalpy of 4.6 J g^{-1} (Fig. 5c). Further, the amorphous polystyrene block exhibits a glass transition T_g of around 107 °C. For P3HT-b-$PPC_{71}BM$ we observe notably broadened peaks showing a melting of P3HT around 211 °C with an enthalpy of 2.3 J g^{-1}. No T_g for the $PC_{71}BM$-grafted polystyrene was observed. The glass transition in such fullerene-grafted polystyrenes is typically shifted toward higher temperature and often shows a strong broadening.[17,38]

To obtain an estimation on the crystallinity of the P3HT segment in the block copolymers, we compared the melting enthalpies with that of neat P3HT, which melts at 230 °C with an enthalpy of 15.1 J g^{-1}. Considering the weight fractions of P3HT in P3HT-b-PS_{OH} and P3HT-b-$PPC_{71}BM$ which are 39 wt% and 28 wt% according to UV-vis in solution, we expect a melting enthalpy of 5.9 and 4.2 J g^{-1} if the same degree of crystallinity as that in the P3HT homopolymer is maintained. The experimentally determined melting enthalpies of 4.6 and 2.3 J g^{-1} are lower and thus indicate a decreased crystallinity of P3HT in both block copolymers as determined in DSC measurements. Since DSC scans are carried out too fast and therefore do not allow for the full crystallization in confined geometries, it is quite natural that the measured ΔH_m values are lower than those expected for the same degree of crystallinity as a homopolymer. This is also in agreement with the varying degree of aggregation depending on annealing conditions observed in UV-vis absorption studies in thin films.

### Structural analysis by X-ray scattering and scanning electron microscopy

Structure formation of the donor–acceptor block copolymer P3HT-b-$PPC_{71}BM$ was investigated using temperature-dependent small-angle X-ray scattering (SAXS) in bulk samples. The morphology of thin films was characterized by scanning electron microscopy (SEM) and grazing-incidence small angle X-ray scattering (GISAXS).

Fig. 6 shows small angle X-ray scattering data obtained from bulk samples of P3HT-b-$PPC_{71}BM$ as measured at 240 °C in the molten state and at room temperature at which P3HT is in a crystalline state. Both scattering curves show a peak in the SAXS range indicating a periodic nanostructure with a periodicity d of about 37 nm at room temperature ($d = 2\pi/q_0$, $q = 0.168$ nm^{-1} at room temperature, $q = 0.16$ nm^{-1} at 240 °C). The fact that the peak is almost unchanged after cooling to room temperature, *i.e.* after crystallization of the P3HT component, suggests that the nanostructure is already caused by a liquid–liquid phase separation in the melt.[14] The weak signal and missing higher order peaks prevent a more detailed analysis of the structure based on X-ray scattering alone. The SEM image shown in Fig. 7 suggests indeed an ordered nanostructure at room temperature of probably cylindrical symmetry. Additionally, there is no indication of the presence of big fullerene aggregates or crystallites. The ordered nanostructure observed in SEM is also consistent with results obtained by
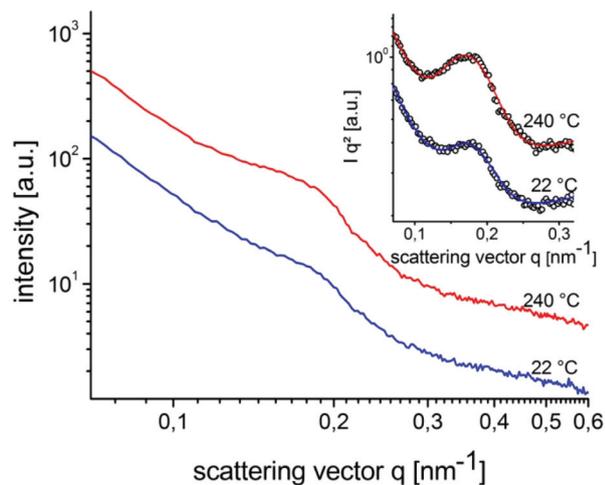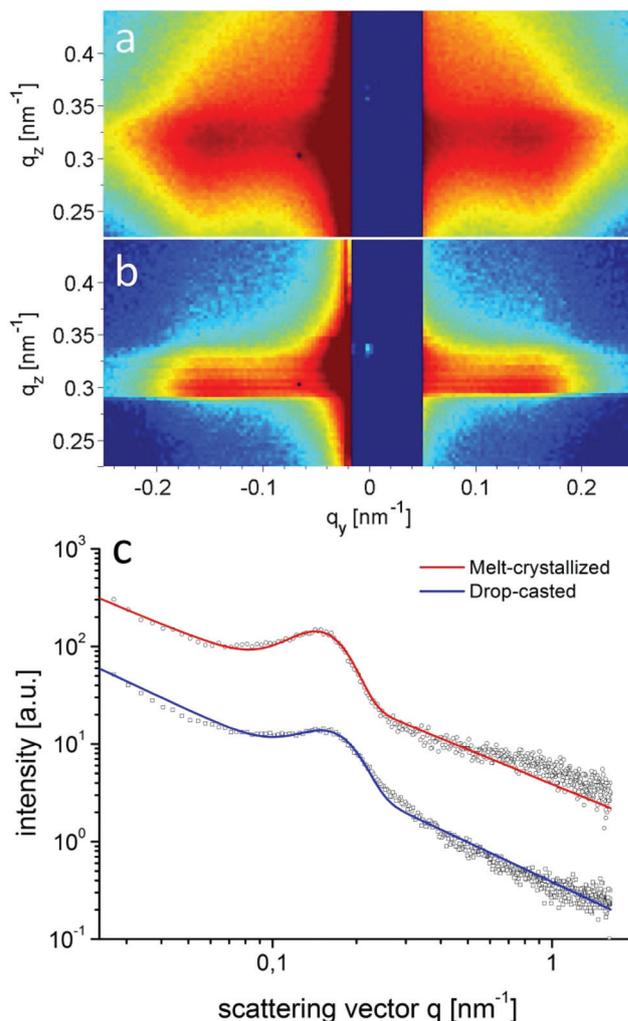
Fig. 6 SAXS intensity of P3HT-*b*-PPC$_{71}$BM at room temperature (blue) and at 240 °C in the melt (red, data set vertically shifted). The inset shows the same data after Lorentz correction with a fit to a model function consisting of a power law background and a Gaussian used to describe the peak.
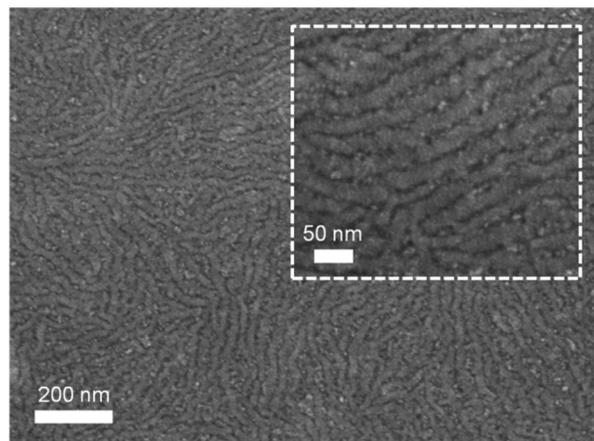
Fig. 7 Scanning electron microscopy image of P3HT-*b*-PPC$_{71}$BM prepared by drop-casting of a 2 wt% dichlorobenzene solution. The inset shows a magnified section of the film.

Fig. 8 2D-GISAXS data of P3HT-*b*-PPC$_{71}$BM around the Yoneda position at room temperature of films prepared by (a) drop-casting and (b) spin-coating with subsequent annealing in the melt. Data in (a) and (b) are displayed on a logarithmic intensity scale. The Yoneda region appears at slightly different nominal q_z values due to a somewhat different angle of incidence. The horizontal intensity profiles of these samples, taken along the Yoneda position, are shown in (c) together with an empirical fit. The peak indicates a periodic nanostructure which is consistent with bulk data (data set of the melt crystallized sample vertically shifted).

GISAXS experiments of thin films as shown in Fig. 8 which show a clear peak indicating a periodic lateral structure within the films. Fig. 8a and b show the corresponding scattering pattern measured in grazing incidence geometry at room temperature for films prepared by drop-casting (Fig. 8a) and by spin-coating with subsequent annealing in the melt (Fig. 8b) respectively. The peak positions in the corresponding horizontal profiles (Fig. 8c) were determined to be $q = 0.146$ nm^{-1} ($d \approx$ 43 nm) for the melt crystallized sample and $q = 0.156$ nm^{-1} ($d \approx 40$ nm) for the drop casted film. Again the peak positions were determined using an empirical model function consisting of a power law background and a Gaussian to describe the peak (see ESI†). Variation of the fitting parameters revealed an uncertainty of about 0.005 nm^{-1} for the peak position. We attribute the small difference in the peak position between the melt crystallized sample and the drop casted film to a solvent remaining in the drop casted film which mediates the incompatibility between both blocks and leads to a smaller structure size.[39] Both samples have the peak at a similar position as the bulk samples indicating that the bulk morphology is largely preserved in thin films. In detail the peak positions in SAXS and GISAXS measurements show a deviation of about 10% probably due to either calibration errors or confinement effects.

The aggregation of fullerene moieties was earlier reported to impede the self-assembly of fullerene-grafted block copolymers into a well-defined nanostructured morphology.[28] However, the presented block copolymer P3HT-*b*-PPC$_{71}$BM

does not show aggregation of fullerene moieties. We attribute this favorable situation to a controlled incorporation of mono-functionalized fullerene moieties. Our observation is further supported by reports of Miyanishi *et al.*[22,40] and Lee *et al.*[25] who also utilized a monofunctionalized fullerene for grafting. In the former, a crystallization driven self-assembly of the fullerene-grafted poly(3-alkylthiophene) block copolymers is suggested to result in a fibril-like surface morphology in thin films. In the latter, phase separation of P3HT-*b*-poly(acrylate) with pendant $PC_{61}BM$ was studied using TEM which indicated phase separation in the range of 10–20 nm. Our findings based on GISAXS and temperature-dependent SAXS clearly show an ordered nanostructure in thin films as well as in the bulk phase of P3HT-*b*-$PPC_{71}BM$.

Conclusions

We demonstrated an elegant synthetic route to $PC_{71}BM$-grafted donor–acceptor block copolymers for the first time using polymer–polymer click chemistry between two tailored polymer blocks followed by a polymer-analogous fullerene grafting. $PC_{71}BM$ grafting was achieved from easily accessible C_{70} carboxylic acid. The covalent incorporation of $PC_{71}BM$ was achieved in very high yields and improves the optical properties of the block copolymer notably. The donor–acceptor block copolymer shows an ordered morphology on the nanoscale in bulk and in thin films independent of the processing method, *i.e.* from solution or by melt crystallization. Further, SAXS and GISAXS structural analysis correlates with the domain size observed in SEM. This pioneering work in the field of $PC_{71}BM$-grafted block copolymers opens new perspectives towards the realization of further fullerene-grafted donor–acceptor block copolymers exploiting the full range of block copolymer morphologies.

Experimental

Materials

The reagents for the following synthetic procedures were purchased from Sigma-Aldrich and used as received, unless stated otherwise. Phenyl-C_{71}-butyric acid methyl ester ($PC_{71}BM$, purity 99%) was purchased from American Dye Source (Canada). Solvents were either distilled at atmospheric pressure utilizing appropriate desiccants or purchased in p.a. (pro analysi) grade. Commercially available anhydrous solvents were purchased from Sigma Aldrich and Acros in sealed bottles with molecular sieves. Prior to polymerization, 4-methoxy-styrene (MS) and 4-*tert*-butoxystyrene (BS) were passed through a column of basic alumina to remove the inhibitor and stored at −18 °C. 2,2,5-Trimethyl-4-phenyl-3-azahexane-3-nitroxide, 2,2,5-trimethyl-3-(1′-*p*-chloromethylphenylethoxy)-4-phenyl-3-azahexane and 2,2,5-trimethyl-3-(1′-*p*-azidomethyl-phenylethoxy)-4-phenyl-3-azahexane were synthesized according to the literature.[41,42] Ethynyl-terminated poly(3-hexylthio-

phene) was prepared by Kumada catalyst transfer polymerization followed by end-capping with ethynylmagnesium chloride.[31] The stock solution of 0.07 M copper(ı) iodide/PMDETA catalyst in tetrahydrofuran was prepared according to a literature procedure.[43]

Instrumentation

^{1}H-NMR spectra were measured with a Bruker Avance AC250 spectrometer at 300 MHz. The obtained spectra were calibrated to the corresponding residual solvent peak ($CDCl_3$ δ = 7.26 ppm, $DMSO-D_6$ δ = 2.50 ppm). Ultraviolet-visible (UV-Vis) spectra from solutions were recorded on a Hitachi U-3000 spectrophotometer using quartz cuvettes with a path length of 1 cm. UV-vis studies of thin films were carried out on a Hitachi U-3000 spectrophotometer and a JASCO Spectrophotometer V-670. The films were prepared by spin-coating from 2 wt% chlorobenzene solution (P3HT and P3HT-*b*-PS_{OH}) or 2.5 wt% 1,2-dichlorobenzene solution (P3HT-*b*-$PPC_{71}BM$) on glass substrates. Fourier transform infrared (FTIR) spectra were recorded from solids on a Perkin Elmer Spectrum 100 FTIR spectrometer in attenuated total reflection (ATR) mode. Thermal gravimetry analysis (TGA) experiments were performed under a continuous nitrogen stream using a Mettler Toledo TGA/SDTA 851. The measurement range was 30–800 °C with a heating rate of 10 K min^{-1}. The determined decomposition temperatures T_{dec} are onset temperatures. Size exclusion chromatography (SEC) with stabilized THF as an eluent was performed using a Waters 515-HPLC pump at a flow rate of 0.5 mL min^{-1}. A guard column (Varian, 50 × 0.75 cm, ResiPore, particle size 3 μm) and two separation columns (Varian, 300 × 0.75 cm, ResiPore, particle size 3 μm) are connected in series with a Waters UV detector at 254 nm and 486 nm. 1,2-Dichlorobenzene (DCB) was used as an internal standard. SEC with chloroform as an eluent was carried out at 25 °C with a FLOM Intelligent Pump 301 at a flow rate of 0.5 mL min^{-1}. A guard column and four separation columns of MZ Analysentechnik with a polystyrene solid phase (particle size 5 μm, pore sizes 10^6, 10^5, 10^3 and 10^2 Å) are connected in series with a Spectra Series UV150 detector at 254 nm and a Shodex RI-71 detector. Toluene was used as an internal standard. High-temperature SEC analysis was carried out on an Agilent (Polymer Laboratories Ltd) PL-GPC 220 high temperature chromatographic unit equipped with DP, RI and LS (15° and 90°) detectors and three linear mixed bed columns of PLgel 13 micrometer (Olexis) with a linear molecular weight operating range: 500–15 000 000 g mol^{-1}. SEC analysis was performed at 150 °C using 1,2,4-trichlorobenzene as the mobile phase. All SEC data were calibrated in relation to polystyrene standards.

Matrix assisted laser desorption ionization mass spectroscopy with time of flight detection (MALDI-TOF MS) was performed on a Bruker Reflex III using either dithranol or *trans*-2-(3-(4-*tert*-butylphenyl)-2-methyl-2-propenylidene)malononitrile (DCTB) as the matrix and, where denoted, silver trifluoroacetate as a cationizing salt. Solutions of the analyte, the matrix and the cationizing salt were prepared, mixed in the given ratio and spotted onto the MALDI target plate. P3HT:

chloroform, dithranol (10 mg mL^{-1}), analyte (0.5 mg mL^{-1}), 50 : 1/v : v. PS$_{OH}$: THF, DCTB (10 mg mL^{-1}), analyte (10 mg mL^{-1}), AgTFA (10 mg mL^{-1}), 20 : 5 : 1/v : v : v. P3HT-*b*-PS$_{OH}$: chloroform, dithranol (10 mg mL^{-1}), analyte (5 mg mL^{-1}), 10 : 2/v : v. P3HT-*b*-PPC$_{71}$BM: chloroform, dithranol (10 mg mL^{-1}), analyte (5 mg mL^{-1}), 20 : 2/v : v.

Small angle X-ray scattering experiments in transmission geometry were performed with a laboratory setup consisting of a Rigaku rotating anode, a focusing X-ray optics device (Osmic confocal max flux), and a Bruker 2D-detector (HI-Star). The optics also served as a monochromator for Cu K$_\alpha$ radiation (λ = 0.154 nm). Aluminum discs with a central hole of 0.8 mm diameter were used as sample holders. The samples were mounted on a Linkam hot stage for temperature control. A heat conducting paste was used to ensure good thermal contact. Grazing incidence small angle X-ray scattering experiments (GISAXS) were performed at the beam line BM 26, DUBBLE, at the ESRF, Grenoble (λ = 0.104 nm). The monochromatic beam was collimated using an assembly of slits and focused on the detector position. An angle of incidence slightly larger than the critical angle of the polymer film and the silicon substrate was used. Rectangular samples had a typical size of 90–140 mm^2 and were completely illuminated by the beam. 2D scattering patterns were collected using a PILATUS 1 M detector. The sample to detector distance was set to 3.07 m. Samples for GISAXS measurements were prepared by spin-coating resp. drop-casting. The spin-coated samples were prepared from a 3 wt% solution in 1,2-dichlorobenzene on silicon substrates at 800 rpm, resulting in a thickness of about 125 nm. After spin-coating the samples were annealed under a nitrogen atmosphere for 90 min at 240 °C and slowly cooled down (approximately 5–10 K min^{-1}). The drop-casted films were prepared from a 3 wt% solution in 1,2-dichlorobenzene, covered with a beaker and dried at room temperature. They had a thickness of about 1.4 μm. The calibration of the SAXS and GISAXS data was performed by comparison with the first order ring of silver behenate measured in transmission.

Scanning electron microscopy (SEM) was performed on a Zeiss LEO 1530 (FE-SEM with the Schottky-field-emission cathode; in-lens detector) using an accelerating voltage of 2.0–3.0 kV. The samples were prepared by drop-casting from a 2 wt% solution in 1,2-dichlorobenzene on indium–tin oxide coated glass substrates, covered with a beaker and slowly dried at room temperature. Spin-casting with quick solvent evaporation and a freezing-in of structures yield shorter structural features. For the SEM measurement the samples were mounted on a standard SEM sample holder by a conductive adhesion graphite-pad (Plano) and sputtered with platinum (2 nm using a Cressington HR208 sputter coater and a Cressington mtm20 thickness controller).

Synthesis procedure of PS

To a dry 10 mL Schlenk tube were added 4-methoxystyrene (4.487 g, 33.44 mmol, 410 eq.), 4-*tert*-butoxystyrene (0.513 g, 2.91 mmol, 36 eq.), 2,2,5-trimethyl-4-phenyl-3-azahexane-3-nitroxide (4 mg, 0.016 mmol, 0.2 eq.) and 2,2,5-trimethyl-3-(1′-

p-azidemethylphenylethoxy)-4-phenyl-3-azahexane (31 mg, 0.081 mmol, 1 eq.) and the mixture was dissolved in 4 mL of dry *o*-dichlorobenzene. The Schlenk tube was sealed with a rubber septum and the reaction mixture was degassed by three freeze, pump and thaw cycles. The polymerization was subsequently started in a preheated oil bath at 125 °C under vigorous stirring. Samples were taken periodically by a syringe to monitor the monomer conversion *via* ^{1}H-NMR spectroscopy. The polymerization was stopped at a conversion of 44% after 550 min by quenching the reaction in liquid nitrogen. The resulting polymer was isolated by precipitation of the reaction mixture three times into 600 mL methanol, filtering the white precipitate and drying under vacuum. Yield: 1.679 g of a white precipitate. ^{1}H-NMR (300 MHz, CDCl$_3$, δ): 7.01–6.09 (br m, 4(a + b)·H, H$_{phenyl}$), 3.95–3.49 (br s, 3b·H, H$_{OMe}$), 2.29–0.97 (br m, 3(a + b)·H, H$_{backbone}$, 9a·H, H$_{OtBu}$). SEC (THF): M_n = 19.6 kg mol^{-1}, M_p = 24.6 kg mol^{-1}, M_w/M_n = 1.19. MALDI: M_p = 23.5 kg mol^{-1}.

Synthesis of PS$_{OH}$

A 250 mL round bottom flask was charged with PS (1.601 g) and dissolved in 160 mL THF. 20 mL of concentrated hydrochloric acid (37 wt%) were added slowly to the solution. After purging the reaction mixture with argon for 20 min *via* a glass pipette, it was stirred at 35 °C for 16 h. All volatile components were removed under reduced pressure. The hydrolyzed polymer was isolated by precipitation twice in 500 mL de-ionized water and freeze-drying from 1,4-dioxane. Yield: 1.29 g of a white precipitate. ^{1}H-NMR (300 MHz, DMSO-d$_6$, δ): 9.25–8.86 (br s, 1a·H, OH), 7.30–5.93 (br m, 4(a + b)·H, H$_{phenyl}$), 3.85–3.45 (br s, 3b·H, H$_{OMe}$), 2.25–0.73 (br m, 3(a + b)·H, H$_{backbone}$). SEC (THF): M_n = 16.7 kg mol^{-1}, M_p = 24.6 kg mol^{-1}, M_w/M_n = 1.19. MALDI: M_p = 24.4 kg mol^{-1}. TGA decomposition T_{dec} = 389 °C.

Synthesis of PPC$_{71}$BM

A 250 ml Schlenk flask was flame dried at 600 °C under high vacuum. It was charged with PS$_{OH}$ (165 mg, 0.124 mmol hydroxy groups, 1 eq.), phenyl-C$_{71}$-butyric acid (250 mg, 0.246 mmol, 2 eq.), and 4-dimethylaminopyridine (49 mg, 0.401 mmol, 3.2 eq). The flask was degassed under high vacuum and backfilled with argon twice. 85 mL of dry *o*-dichlorobenzene was added and the mixture was ultrasonicated for 30 min at room temperature. In a separate 50 mL Schlenk flask under argon, *N*,*N*′-dicyclohexylcarbodiimide (178 mg, 0.862 mmol, 7 eq.) was dissolved in 15 mL of dry *o*-dichlorobenzene. Then the DCC solution was added dropwise to the reaction mixture, which was then stirred at 40 °C for 23 h. After removal of the solvents under reduced pressure at 60 °C, the crude product was redissolved in DCB and filtered. For polymer purification the filtrate was precipitated first in 500 mL methanol, then three times in 500 mL of methanol–toluene (2 : 1, v : v) and finally in 500 mL methanol. The purity of the obtained polymer was monitored by TLC (SiO$_2$, toluene), where the polymer remains on the start line and the impurities show distinct spots. The precipitate was

dried under high vacuum. Yield: 210 mg of a deep brown precipitate. ^{1}H-NMR (300 MHz, CDCl$_3$, δ): 8.11–7.72 (br m, 2a·H, Ph–C–(CH$_2$)$_3$–COOR), 7.65–7.33 (br m, 3·aH, Ph–C–(CH$_2$)$_3$–COOR), 7.08–5.97 (br m, 4(a + b)·H, H$_{phenyl}$), 3.99–3.49 (br s, 4b·H, H$_{OMe}$), 2.79–2.61,2.61–2.44 (br m, 4a·H, Ph–C–CH_2–CH$_2$–CH_2–COOR), 2.36–0.94 (br m, 2aH, Ph–C–CH$_2$–CH_2–CH$_2$–COOR, 3(a + b)H, H$_{backbone}$). SEC (CHCl$_3$): M_n = 20.8 kg mol^{-1}, M_p = 26.3 kg mol^{-1}, M_w/M_n = 1.27. MALDI: M_p = 42.5 kg mol^{-1}. TGA decomposition T_{dec} = 390 °C.

Synthesis of PS-Cl

To a dry 10 mL Schlenk tube were added 4-methoxystyrene (4.482 g, 33.41 mmol, 260 eq.), 4-tert-butoxystyrene (0.511 g, 2.91 mmol, 23 eq.), 2,2,5-trimethyl-4-phenyl-3-azahexane-3-nitroxide (6 mg, 0.026 mmol, 0.2 eq.) and 2,2,5-trimethyl-3-(1′-p-chloromethylphenylethoxy)-4-phenyl-3-azahexane (48.2 mg, 0.129 mmol, 1 eq.). The Schlenk tube was sealed with a rubber septum and the reaction mixture was degassed by three freeze, pump and thaw cycles. The polymerization was subsequently started in a preheated oil bath at 125 °C under vigorous stirring. Samples were taken periodically by a syringe to monitor the monomer conversion via ^{1}H-NMR spectroscopy. The polymerization was stopped at a conversion of 40% after 410 min by quenching the reaction in liquid nitrogen. The resulting polymer was isolated by precipitation of the reaction mixture three times in 600 mL methanol, filtering the white precipitate and drying under vacuum. Yield: 1.593 g of a white precipitate. ^{1}H-NMR (300 MHz, CDCl$_3$, δ): 6.95–6.15 (br m, 4(a + b)·H, H$_{phenyl}$), 3.90–3.56 (br s, 3b·H, H$_{OMe}$), 2.25–0.85 (br m, 3(a + b)·H, H$_{backbone}$, 9a·H, H$_{OtBu}$). SEC (THF): M_n = 10.7 kg mol^{-1}, M_w/M_n = 1.10.

Synthesis of PS-Az

A dry Schlenk flask was charged with PS-Cl (1.30 g, approximately 0.07 mmol, 1 eq.) and sodium azide (0.11 g, 1.69 mmol, 24 eq.) and sealed with a rubber septum. It was degassed under high vacuum and backfilled with argon three times before adding dry N,N-dimethylformamide (20 mL) via a syringe. The suspension was stirred for 70 h at room temperature. The polymer was isolated by diluting the reaction mixture with a small amount of THF and precipitation in 600 mL deionized water twice. After filtering the white precipitate, it was washed with 100 mL methanol and dried in a vacuum at room temperature. Yield: 1.223 g of a white precipitate. ^{1}H-NMR (300 MHz, CDCl$_3$, δ): 6.96–6.14 (br m, 4(a + b)·H, H$_{phenyl}$), 3.87–3.59 (br s, 3b·H, H$_{OMe}$), 2.25–0.83 (br m, 3(a + b)·H, H$_{backbone}$, 9a·H, H$_{OtBu}$). SEC (THF): M_n = 10.4 kg mol^{-1}, M_w/M_n = 1.10.

Synthesis of PS$_{OH}$-Az

A 250 mL round bottom flask was charged with PS-Az (1.10 g) and dissolved in 110 mL THF. 13.8 mL of concentrated hydrochloric acid (37 wt%) were added slowly to the solution. After purging the reaction mixture with argon for 20 min via a glass pipette, it was stirred at 35 °C for 20 h. For work-up, all volatile components were removed under reduced pressure. The hydro-

lyzed polymer was isolated by precipitation twice in 600 mL deionized water and freeze-drying from 1,4-dioxane. Yield: 0.92 g of a white precipitate. ^{1}H-NMR (300 MHz, DMSO-d$_6$, δ): 9.28–8.83 (br s, 1a·H, OH), 7.10–5.97 (br m, 4(a + b)·H, H$_{phenyl}$), 3.80–3.51 (br s, 3b·H, H$_{OMe}$), 2.315–0.72 (br m, 3(a + b)·H, H$_{backbone}$). SEC (THF): M_n = 9.8 kg mol^{-1}, M_p = 11.4 kg mol^{-1}, M_w/M_n = 1.11. MALDI: M_p = 13.4 kg mol^{-1}.

Synthesis of P3HT-b-PS$_{OH}$

A dry 20 mL Schlenk tube with a screw cap was charged with P3HT-alkyne (75 mg, approx. 6.1 µmol, 1 eq.) and PS$_{OH}$-Cl (223 mg, approx. 16.6 µmol, 2.7 eq.). It was degassed under high vacuum and backfilled with argon three times. 20 mL of dry THF were added under argon and the solution was stirred for 20 min at 50 °C until all components were fully dissolved. After purging the mixture with argon via a needle for 20 min, the copper iodide/PMDETA catalyst solution (0.5 mL, 0.07 M, 35 µmol) was added under argon. The Schlenk flask was sealed with the screw cap and cautiously degassed under vacuum and backfilled with argon three times to remove any oxygen traces. The reaction mixture was stirred for 26 h at 50 °C, 0.3 mL of the catalyst solution was added and the solution was stirred for another 17 h. The reaction mixture was passed through a short column of basic aluminium oxide to remove the copper catalyst. The column was washed with 50 mL of THF, the organic fractions were combined and the solvent was removed under reduced pressure. The polymer was isolated by precipitation twice in 300 mL of methanol–acetone (2 : 1, v : v) from THF and drying the precipitate under vacuum at room temperature. Yield: 163 mg of a black precipitate. ^{1}H-NMR (300 MHz, o-DCB-d$_4$, δ): 7.37 (s, m·1H, H$_a$), 7.10–6.55 (br m, n·4(a + b)·H, H$_{phenyl}$), 4.00–3.66 (br s, n·3b·H, H$_{OMe}$), 3.20–2.96 (br m, m·2H, H$_b$), 2.00–1.85 (br m, H$_c$), 1.68–1.55 (br m, H$_d$), 1.54–1.38 (br m, H$_e$, H$_f$), 2.38–1.34 (br m, H$_{backbone}$), 1.10 (tr, m·3H, H$_g$). SEC (CHCl$_3$): M_n = 26.3 kg mol^{-1}, M_p = 35.4 kg mol^{-1}, M_w/M_n = 1.10. MALDI: M_p = 25.9 kg mol^{-1}.

Synthesis of P3HT-b-PPC$_{71}$BM

A 100 ml Schlenk flask was flame dried at 600 °C under high vacuum. It was charged with P3HT-b-PS$_{OH}$ (50 mg, approx. 1.9 µmol polymer, 19 µmol hydroxy groups, 1 eq.), phenyl-C$_{71}$-butyric acid (49 mg, 48 µmol, 2.5 eq.), and 4-dimethylamino-pyridine (9 mg, 68.6 µmol, 3.6 eq.). The flask was degassed under high vacuum and backfilled with argon twice. 17 mL of dry o-dichlorobenzene were added and the mixture was ultrasonicated for 30 min at room temperature. In a separate 10 mL Schlenk flask under argon, N,N′-dicyclohexylcarbodiimide (33 mg, 160 µmol, 8.4 eq.) was dissolved in 3 mL of dry o-dichlorobenzene. Then the DCC solution was added dropwise to the reaction mixture, which was then stirred at 40 °C for 23 h. After removal of the solvents under reduced pressure at 60 °C, the crude product was redissolved in chloroform and filtered. For polymer purification the filtrate was precipitated first in 300 mL methanol–toluene (1 : 1, v : v) twice and then in 300 mL methanol. The purity of the obtained polymer was monitored by TLC (SiO$_2$, toluene), where the polymer remains

on the start line and the impurities show distinct spots. The precipitate was dried under vacuum at room temperature. Yield: 61 mg of a black precipitate. ^{1}H-NMR (300 MHz, o-DCB-d$_4$, δ): 7.94–7.87, 7.70–7.44 (br m, H$_h$, H$_i$), 7.36 (s, m·1H, H$_a$), 7.09–6.55 (br m, n·4(a + b)·H, H$_{phenyl}$), 3.98–3.68 (br s, n·3b·H, H$_{OMe}$), 3.22–2.95 (br m, m·2H, H$_b$), 2.01–1.84 (br m, H$_c$), 1.69–1.55 (br m, H$_d$), 1.54–1.36 (br m, H$_e$, H$_f$), 2.07–1.24 (br m, H$_{backbone}$), 1.09 (m, m·3H, H$_g$). SEC (CHCl$_3$): M_n = 27.5 kg mol^{-1}, M_p = 36.6 kg mol^{-1}, M_w/M_n = 1.31. MALDI: M_p = 31.5 kg mol^{-1}.

Acknowledgements

Notes and references

1 K. M. Coakley and M. D. McGehee, *Chem. Mater.*, 2004, **16**, 4533–4542.

2 J. Peet, M. L. Senatore, A. J. Heeger and G. C. Bazan, *Adv. Mater.*, 2009, **21**, 1521–1527.

3 G. Yu, J. Gao, J. C. Hummelen, F. Wudl and A. J. Heeger, *Science*, 1995, **270**, 1789–1791.

4 J. K. J. van Duren, X. Yang, J. Loos, C. W. T. Bulle-Lieuwma, A. B. Sieval, J. C. Hummelen and R. A. J. Janssen, *Adv. Funct. Mater.*, 2004, **14**, 425–434.

5 W. Ma, C. Yang, X. Gong, K. Lee and A. J. Heeger, *Adv. Funct. Mater.*, 2005, **15**, 1617–1622.

6 T. Erb, U. Zhokhavets, G. Gobsch, S. Raleva, B. Stühn, P. Schilinsky, C. Waldauf and C. J. Brabec, *Adv. Funct. Mater.*, 2005, **15**, 1193–1196.

7 J. U. Lee, J. W. Jung, T. Emrick, T. P. Russell and W. H. Jo, *Nanotechnology*, 2010, **21**, 105201.

8 S. Bertho, G. Janssen, T. J. Cleij, B. Conings, W. Moons, A. Gadisa, J. D'Haen, E. Goovaerts, L. Lutsen, J. Manca and D. Vanderzande, *Sol. Energy Mater. Sol. Cells*, 2008, **92**, 753–760.

9 F. C. Krebs, *Sol. Energy Mater. Sol. Cells*, 2009, **93**, 394–412.

10 M. W. Matsen and F. S. Bates, *Macromolecules*, 1996, **29**, 1091–1098.

11 M. Shah and V. Ganesan, *Macromolecules*, 2010, **43**, 543–552.

12 P. D. Topham, A. J. Parnell and R. C. Hiorns, *J. Polym. Sci., Part B: Polym. Phys.*, 2011, **49**, 1131–1156.

13 M. Sommer, S. Huettner and M. Thelakkat, *J. Mater. Chem.*, 2010, **20**, 10788.

14 R. H. Lohwasser, G. Gupta, P. Kohn, M. Sommer, A. S. Lang, T. Thurn-Albrecht and M. Thelakkat, *Macromolecules*, 2013, **46**, 4403–4410.

15 U. Stalmach, B. de Boer, C. Videlot, P. F. van Hutten and G. Hadziioannou, *J. Am. Chem. Soc.*, 2000, **122**, 5464–5472.

16 L. Perrin, A. Nourdine, E. Planes, C. Carrot, N. Alberola and L. Flandin, *J. Polym. Sci., Part B: Polym. Phys.*, 2013, **51**, 291–302.

17 M. Hufnagel, M.-A. Muth, J. C. Brendel and M. Thelakkat, *Macromolecules*, 2014, **47**, 2324–2332.

18 B. de Boer, U. Stalmach, P. F. van Hutten, C. Melzer, V. V. Krasnikov, G. Hadziioannou, B. De Boer and P. F. Van Hutten, *Polymer*, 2001, **42**, 9097–9109.

19 M. H. van der Veen, B. de Boer, U. Stalmach, K. I. van de Wetering and G. Hadziioannou, *Macromolecules*, 2004, **37**, 3673–3684.

20 B. Gholamkhass and S. Holdcroft, *Chem. Mater.*, 2010, **22**, 5371–5376.

21 C. Yang, J. K. Lee, A. J. Heeger and F. Wudl, *J. Mater. Chem.*, 2009, **19**, 5416–5423.

22 S. Miyanishi, Y. Zhang, K. Hashimoto and K. Tajima, *Macromolecules*, 2012, **45**, 6424–6437.

23 X.-H. Dong, W.-B. Zhang, Y. Li, M. Huang, S. Zhang, R. P. Quirk and S. Z. D. Cheng, *Polym. Chem.*, 2012, **3**, 124–134.

24 M. Heuken, H. Komber, T. Erdmann, V. Senkovskyy, A. Kiriy and B. Voit, *Macromolecules*, 2012, **45**, 4101–4114.

25 J. U. Lee, A. Cirpan, T. Emrick, P. Russell, W. Ho, T. P. Russell and W. H. Jo, *J. Mater. Chem.*, 2009, **19**, 1483–1489.

26 J. C. Hummelen, B. W. Knight, F. LePeq, F. Wudl, J. Yao and C. L. Wilkins, *J. Org. Chem.*, 1995, **60**, 532–538.

27 K. Sivula, Z. T. Ball, N. Watanabe and J. M. J. Fréchet, *Adv. Mater.*, 2006, **18**, 206–210.

28 S. Barrau, T. Heiser, F. Richard, C. Brochon, C. Ngov, K. van de Wetering, G. Hadziioannou, D. V. Anokhin and D. A. Ivanov, *Macromolecules*, 2008, **41**, 2701–2710.

29 M. M. Wienk, J. M. Kroon, W. J. H. Verhees, J. Knol, J. C. Hummelen, P. A. van Hal and R. A. J. Janssen, *Angew. Chem., Int. Ed.*, 2003, **42**, 3371–3375.

30 Z. He, C. Zhong, S. Su, M. Xu, H. Wu and Y. Cao, *Nat. Photonics*, 2012, **6**, 593–597.

31 R. H. Lohwasser and M. Thelakkat, *Macromolecules*, 2012, **45**, 3070–3077.

32 C. J. Brabec, S. Gowrisanker, J. J. M. Halls, D. Laird, S. Jia and S. P. Williams, *Adv. Mater.*, 2010, **22**, 3839–3856.

33 E. Lieber, C. N. R. Rao, T. Chao and C. Hoffman, *Anal. Chem.*, 1957, **29**, 916–918.

34 S. Fleischmann, H. Komber, D. Appelhans and B. I. Voit, *Macromol. Chem. Phys.*, 2007, **208**, 1050–1060.

35 C. R. Singh, G. Gupta, R. Lohwasser, S. Engmann, J. Balko, M. Thelakkat, T. Thurn-Albrecht and H. Hoppe, *J. Polym. Sci., Part B: Polym. Phys.*, 2013, **51**, 943–951.

36 M. Thelakkat, P. Pösch and H. W. Schmidt, *Macromolecules*, 2001, **34**, 7441–7447.

37 F. C. Spano, *J. Chem. Phys.*, 2005, **122**, 234701.

38 C. J. Hawker, *Macromolecules*, 1994, **27**, 4836–4837.

39 A. Knoll, R. Magerle and G. Krausch, *J. Chem. Phys.*, 2004, **120**, 1105–1116.

40 S. Miyanishi, Y. Zhang, K. Tajima and K. Hashimoto, *Chem. Commun.*, 2010, **46**, 6723–6725.

41 A. W. Bosman, R. Vestberg, A. Heumann, J. M. J. Fréchet and C. J. Hawker, *J. Am. Chem. Soc.*, 2003, **125**, 715–728.

42 W. Binder, D. Gloger, H. Weinstabl, G. Allmaier and E. Pittenauer, *Macromolecules*, 2007, **40**, 3097–3107.

43 A. S. Lang and M. Thelakkat, *Polym. Chem.*, 2011, **2**, 2213.